

STEADY STATE SIMULATION OF HEAT PIPES IN CRITICAL CONDITIONS OF HEAT FLUX AND ROTATION

Humberto Araujo Machado – machado@univap.br

Universidade do Vale do Paraíba, UNIVAP - IP&D

Av Shishima Hifume, 2911, 12244-000, São José dos Campos, SP, Brazil

Ricardo Fortes de Miranda- rfmiranda@mecanica.ufu.br

Universidade Federal de Uberlândia, Faculdade de Engenharia Mecânica

Campus Santa Mônica, bloco 1M, 38400-902, Uberlândia, MG, Brazil.

***Abstract.** Rotating circular heat pipes have some important applications, as electric engines cooling, turbine thermal control, etc. The effect of rotation in its work becomes important in both critical cases, when the angular velocity or heat flux are too large, compared to the heat transfer and fluid flow scales. In this work, a steady rotating cylindrical heat pipe is simulated through the finite volume method, coupling the vapor zone and porous media. Several values for angular and linear Reynolds number, as functions of angular velocity and heat flux, respectively, are showed, as well the effects of such variation in the streamlines of the whole heat pipe dominium. A limit for heat pipe operation, taking into account the losses of heat exchange capacity, is presented as a curve related to the Reynolds numbers, which can be useful for heat pipe design.*

***Key-words:** Rotating heat pipes, Finite volume, Phase change in porous media*

1. INTRODUCTION

Rotating Heat Pipes are a good option to refrigerate rotating equipment, as electrical engines and turbines, where they are normally mounted in the machine axis. They present many advantages when compared to conventional cooling systems. In satellites, space crafts and space probes, where commonly a spin movement appears, space heat pipe design should keep its cooling capacity, despite of rotation, since they are crucial to relieve the heat excess in the chip system.

Such devices can transport the heat continuously, if the porous media does not get dry, which will occur if the flow is blocked or the capillary pressure is not high enough. The rotation will oppose to the flow in the radial direction at the evaporator section, due the centrifugal force, when the vapor leaves the limit of porous section and goes to the condenser section, in tubes mounted into the axis. If the rotation is high enough, the phase change stops, and the heat exchange will occurs only by convection which makes the heat pipe efficiency decreases highly. Even if the process of evaporation is not interrupted, the excess of rotation or wall heat flux yields one or more recirculation zones in the vapor section, reducing the heat

exchange as well. This behavior is not captured by empirical or simple analytical models, like that proposed by Daniels & Al-Jumaily (1973) and Daniels & Williams (1978,1979).

Ismail & Miranda (1988) presented a two dimensional model for cylindrical rotating heat pipes, for rotations up to 3600 rpm and the results indicated a limiting rotation, when the heat pipe breaks down. Faghri et al. (1993) investigated heat pipes with radial Reynolds number from 0,01 to 0.20, and radial speed to 2800 rpm, confirming the presence of recirculations below of a certain rotation. Harley e Faghri (1995) presented a two-dimensional model for conical rotating heat pipes. Ismail & Miranda (1997) presented also a two-dimensional model for rotating cylindrical heat pipes with porous structure, which was complemented by Miranda (1998). In that work, the effects of the heat flux over the velocity of injection and the whole flow where explored for several pipe diameters and radial speeds, as a tentative to find the optimal point of operation.

In this work, the model of Miranda (1998) is extended to the porous region, and the effects of increasing heat flux and rotation over the pipe flow and heat exchange are analyzed. An interpolated curve $Re_{radial} \times Re_{axial}$ is showed as the upper limit of the rotation.

2. MATHEMATICAL FORMULATION

Considering a cylindrical pipe with constant angular velocity Ω in steady state operation, submitted to a wall heat flux Q in a half section and $-Q$ in the other, represented in a axisymmetric cylindrical coordinate system (Fig. 1).

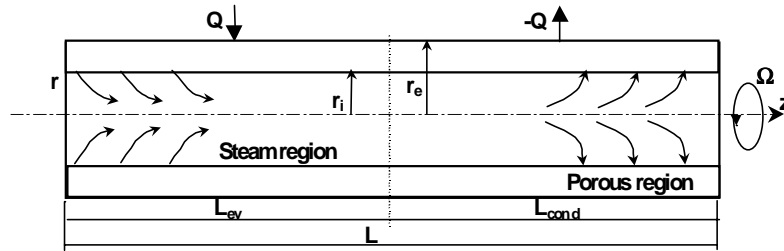


Figure 1. Schematic view of a rotating heat pipe.

Assuming that both phases are incompressible and have constant physical properties under laminar flow, each one is represented by the following set of equations:

$$\frac{\partial V}{\partial r} + \frac{V}{r} + \frac{\partial U}{\partial z} = 0 \quad (1)$$

$$\rho \left(V \frac{\partial V}{\partial r} - \frac{V^2}{r} + U \frac{\partial V}{\partial z} \right) = -\varepsilon \frac{\partial P}{\partial r} + \mu \left(\frac{\partial^2 V}{\partial r^2} + \frac{1}{r} \frac{\partial V}{\partial r} - \frac{V}{r} + \frac{\partial^2 V}{\partial z^2} \right) - \frac{\mu \varepsilon}{K} V + 2\rho \Omega W + \rho \Omega^2 r \quad (2)$$

$$\rho \left(V \frac{\partial W}{\partial r} - \frac{W^2}{r} + U \frac{\partial W}{\partial z} \right) = \mu \left(\frac{\partial^2 W}{\partial r^2} + \frac{1}{r} \frac{\partial W}{\partial r} - \frac{W}{r} + \frac{\partial^2 W}{\partial z^2} \right) - \frac{\mu \varepsilon}{K} W + 2\rho \Omega V \quad (3)$$

$$\rho \left(V \frac{\partial U}{\partial r} + U \frac{\partial U}{\partial z} \right) = -\varepsilon \frac{\partial P}{\partial z} + \mu \left(\frac{\partial^2 U}{\partial r^2} + \frac{1}{r} \frac{\partial U}{\partial r} + \frac{\partial^2 U}{\partial z^2} \right) - \frac{\mu \varepsilon}{K} U \quad (4)$$

$$V \frac{\partial T}{\partial r} + U \frac{\partial T}{\partial z} = \alpha \left(\frac{\partial^2 T}{\partial r^2} + \frac{1}{r} \frac{\partial T}{\partial r} + \frac{\partial^2 T}{\partial z^2} \right) \quad (5)$$

where U , W and V are the axial, longitudinal and radial velocity components, respectively. In the vapor region, the porosity is considered to be $\varepsilon = 1$ and the permeability $K \rightarrow \infty$. The boundary conditions are:

$$V = W = U = 0; \quad \frac{\partial T}{\partial z} = 0 \quad \text{at } z = 0 \text{ and } z = L \quad (6.a)$$

$$V = W = 0; \quad \frac{\partial U}{\partial z} = 0; \quad \frac{\partial T}{\partial z} = 0 \quad \text{at } r = 0 \quad (6.b)$$

$$V = V_i(z); \quad W = U = 0; \quad T = T_{sat} \quad \text{at } r = r_i \quad (6.c)$$

$$V = W = U = 0; \quad -k \frac{\partial T}{\partial r} = Q \text{ in } z > 0.5, \quad -Q \text{ in } z < 0.5 \quad \text{at } r = r_w \quad (6.d)$$

where $V_i(z)$ is the local velocity of injection, that couples the vapor and porous regions, and is found along the solution, via numerical iterations.

3. RESULTS

The equations were solved by the finite volume method, applied to a 202 x 82 displaced mesh. The pressure-velocity coupling was made through the SIMPLE algorithm, and the program runs in PC Pentium 200 MHz. The simulations were done for water as working fluid and a reference pressure used was $1.0197 \times 10^5 \text{ N/m}^2$. Tube dimensions were $r_w = 0.02 \text{ m}$, $L = 1 \text{ m}$ and $r_i = 0.0127 \text{ m}$. The porous media matrix was copper, with $K = 0.358 \times 10^{-8} \text{ m}^2$ and $\varepsilon = 0.446$. Results were obtained for $\Omega = 0, 5, 10, 30, 60, 100, 200 \text{ rps}$, using $Q = 10^2, 5 \times 10^2, 10^3, 5 \times 10^3, 10^4, 5 \times 10^4, 10^5, 1.5 \times 10^5 \text{ W/m}^2$. The presence of rotation implies that the vapor must surmount the centrifugal force in order to reach condenser. If vapor kinetic energy is not enough, the critical condition is reached, and the flow is blocked, inducing the heat pipe operation collapse (Miranda, 1998). In this sense, any loss in the flow, as recirculations or instabilities, is a cause for reduction of heat pipe efficiency.

Figure 2 shows the appearing and evolution of recirculation cells for $Q = 100 \text{ W/m}^2$. The cells seem to be open or cut, but they are closed very close to the wall. Initially, in $\Omega = 10$ (Fig. 2.a), the circulation is almost perfectly symmetrical. In $\Omega = 60$ (Fig. 2.b), a recirculation cell appears at the left boundary, which is the region where the centrifugal force offers the highest resistance to the flow. Such recirculation grows, from $\Omega = 60$ to 100 (Fig. 2.c), and at $\Omega = 200$ (Fig. 2.d) it occupies a lot of the left side of the vapor zone, and another one appears in the right side. In this case, vapor suffers high acceleration forward to the condenser, and its edge is not able to absorb such vapor flux. The circulation from the porous to the vapor zone is greatly reduced, limited to a small place close to the boundary between the zones. Obviously, in this case the amount of fluid able to transport heat is a fraction of the total. Such recirculation cells are a consequence of resistance to the flow, caused by the centrifugal force. Vapor encounters difficulties to leave the evaporator section in the radial direction, but it is accelerated to the condenser section, and as the rotation rises, both effects are combined, yielding the instabilities that will produce the recirculations. The extreme case is the complete stop of the thermal cycle, when the vapor and liquid will circulate only in their own zone, transforming

the heat exchange in a simple convection heat transfer process. This process seems to appear up to 200 rps. Miranda (1998) has observed that, the simulation without the porous media coupling becomes unstable at lower rotation (60 rps). Such effect can be a consequence of some stabilization provided by the porous media flow, and deserves more study.

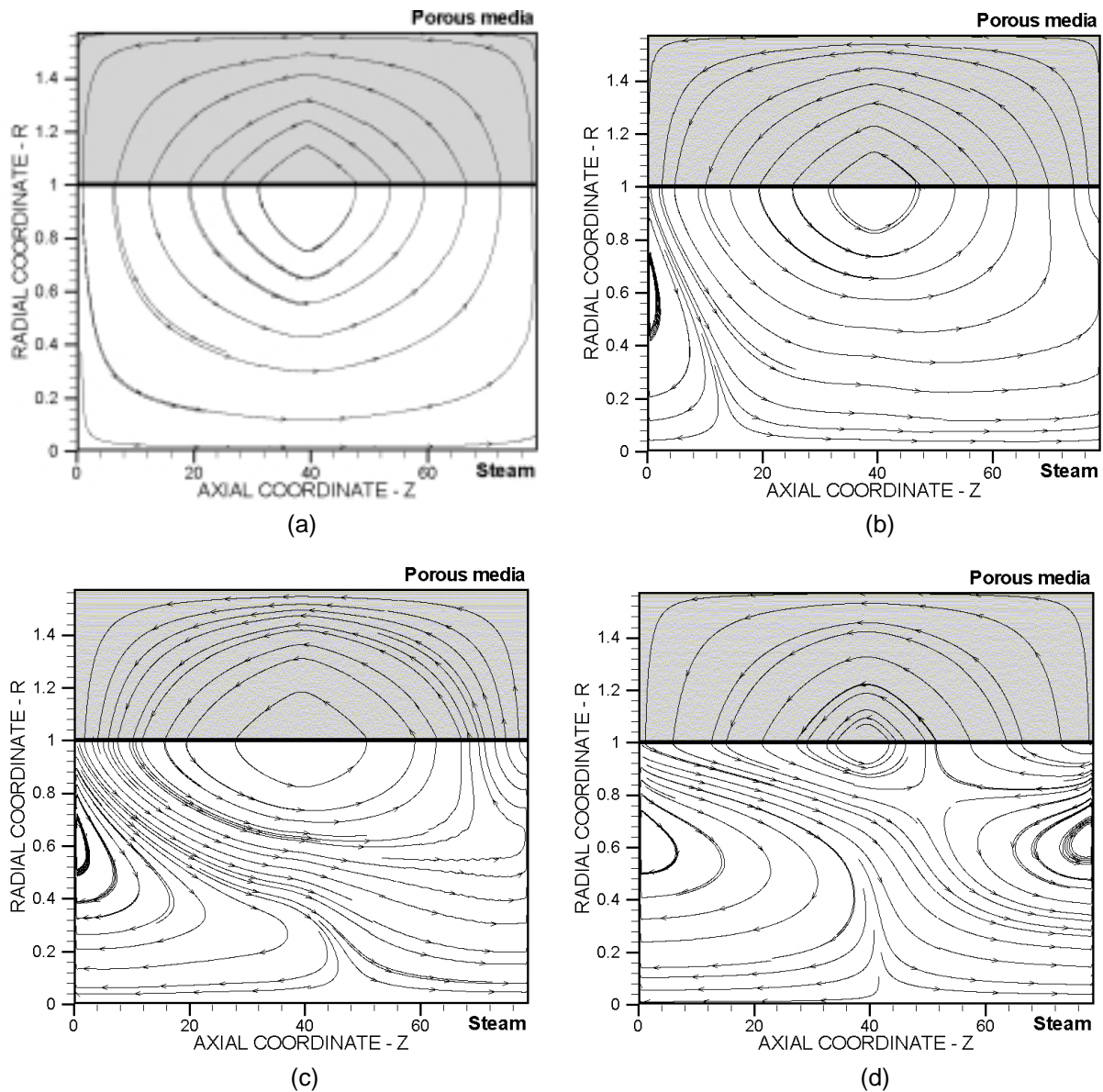


Figure 2. Streamlines, $Q = 100$: (a) $\Omega = 10$, (b) $\Omega = 60$, (c) $\Omega = 100$, (d) $\Omega = 200$.

Figure 3 shows the flow evolution with the increase in heat flux when $\Omega = 60$. In this case the flow is more stable, and recirculation starts at the right boundary. The reason is that the heat flux is enough to win the centrifugal force in the evaporator section but, at the condenser section, the vapor is accelerated due this force and must be strongly decelerate close to the wall. Such excess of momentum becomes an instability, and generate the vortex cell. At $Q = 10^4$, the flow is still equilibrated (Fig. 3.a). At $Q = 5 \times 10^4$, the first recirculation appears, and become two at $Q = 10^5$. At $Q = 1.5 \times 10^5$ the cells seen to join themselves, occupying a smaller place. But the closer streamlines indicate that the deceleration is stronger, that means a major fraction of total vapor energy spent in the recirculation.

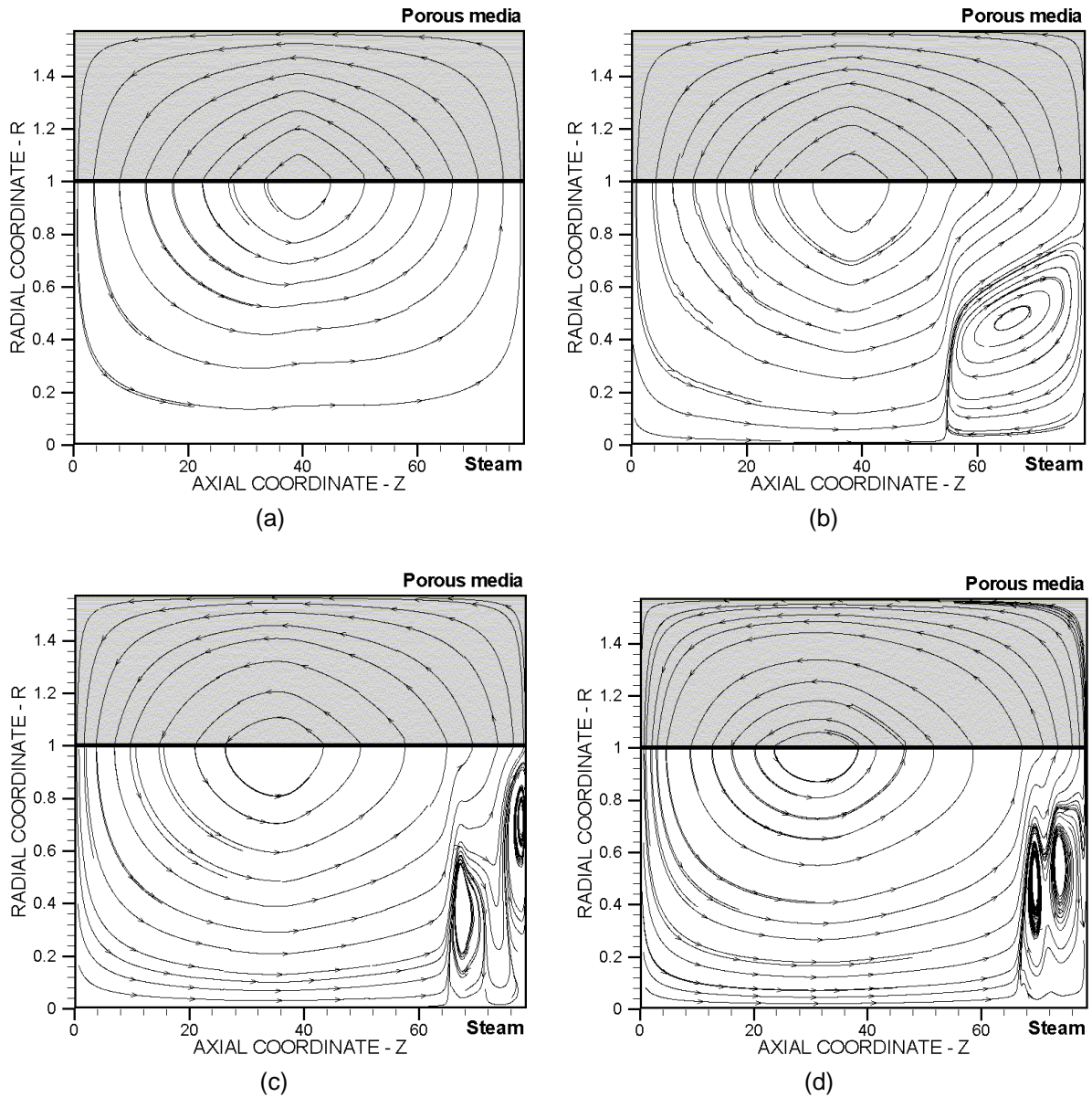


Figure 3. Streamlines, $\Omega = 60$: (a) $Q = 10^4$, (b) $Q = 5 \times 10^4$, (c) $Q = 10^5$, (d) $Q = 1.5 \times 10^5$.

Figure 4 shows the evolution of vapor pressure field for $\Omega = 60$, since the liquid pressure field does not change its shape with the rotation (Fig. 4.a). At higher heat flux, it is possible to observe the “valley” between the evaporator and condenser section (Fig. 4.b), and a small perturbation in the recirculating region as well. In these conditions, the pressure variation is strongly coupled to the axial velocity, very close to the simple Bernoulli equation. The valley begins to vanish by its borders as the heat flux reduces (Figs. 4.c-e). At a very low heat flux, where a recirculation in the opposite side already appears, the difference of pressure between the sections is not significant, and the main pressure difference is imposed by the centrifugal force (Fig. 4.f). It seems realistic, since the heat flux produces very small axial velocities, and the pressure must equilibrate the centrifugal force induced by rotation.

Axial velocity profiles correspond to pressure behavior in high heat fluxes, and are more regular as the rotation rises and heat flux decreases. In Figs. 5.a and 5.c the recirculations observed in stream functions can be seen as deformations in U-profiles as a consequence of the extreme deceleration and change in the direction suffered by the fluid when it gets close to

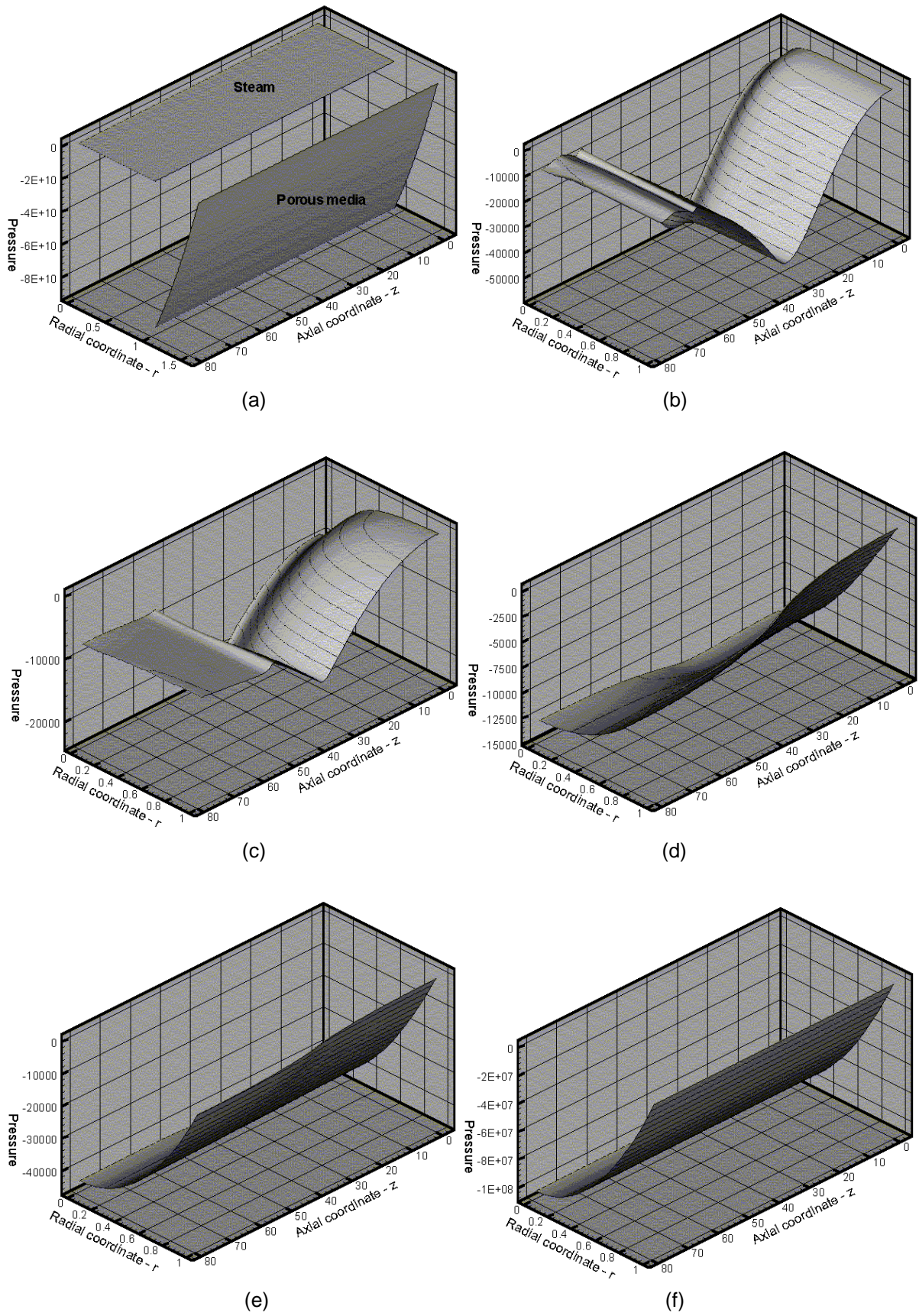


Figure 4. Pressure fields, $\Omega = 60$: (a) vapor and liquid, $Q = 10^5$, vapor only: (b) $Q = 10^5$, (c) $Q = 5 \times 10^4$, (d) $Q = 10^4$, (e) $Q = 5 \times 10^3$, (f) $Q = 10^2$.

the wall at the condenser section, due its high kinetic energy. Such deformations become smooth in lower fluxes (Figs. 5.b, 5.d), but they still exist. As the heat flux decreases, the profile becomes more regular, because the pressure variation induced by the centrifugal force is high enough the stabilize the flow, and deformation in this case correspond to recirculation induced by centrifugal force at the evaporator section.

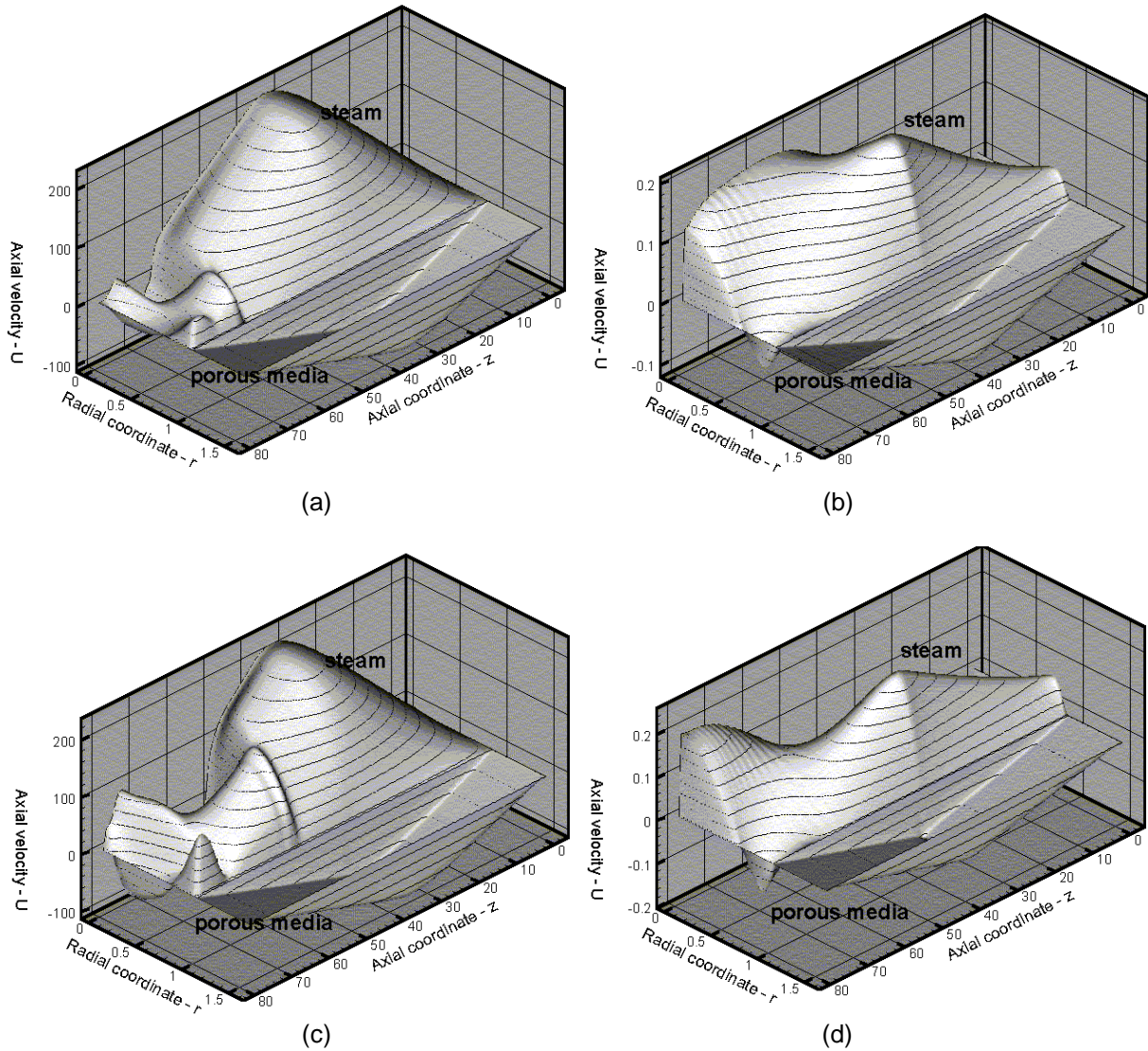


Figure 5. Axial velocity, $\Omega = 60$: (a) $Q = 10^5$, (b) $Q = 10^2$; $\Omega = 100$: (d) $Q = 10^5$, (e) $Q = 10^2$.

Radial velocity profiles are more regular, since its order is lower than the axial component. In a higher heat flux, some “hills” appear in recirculations, which is several orders higher than the average value (Fig. 6.a), that indicates some flow instability. At low fluxes the protuberances appear in both extremes, due the low energy of the fluid close to the walls, and they indicate that the vapor is accelerated to the center (Fig. 6.b), since its values are positive. As a comparison, the velocity profiles for $\Omega = 0$ are shown in Figs. 7.a-b, where one can see the perfect symmetry among each regions.

An important parameter for heat pipe design is the maximum temperature reached by the liquid in porous media. The perfect working of the heat pipe is supposed to happen in absence of boiling nucleation, which occurs about 1.3°C plus the saturation temperature (here

considered 100^0 C). Since it can be even worse than the recirculations caused by the excess of heat fluxes, and may dry the heat pipe, it is necessary to investigate what will happens first.

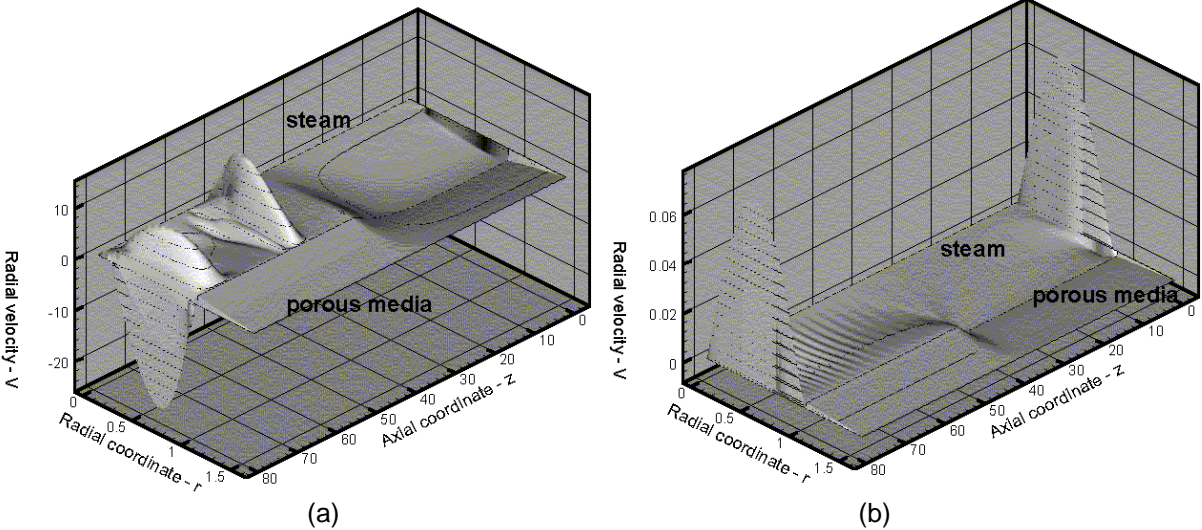


Figure 6. Radial velocity - V , $\Omega = 100$: (a) $Q = 10^5$, (b) $Q = 10^2$.

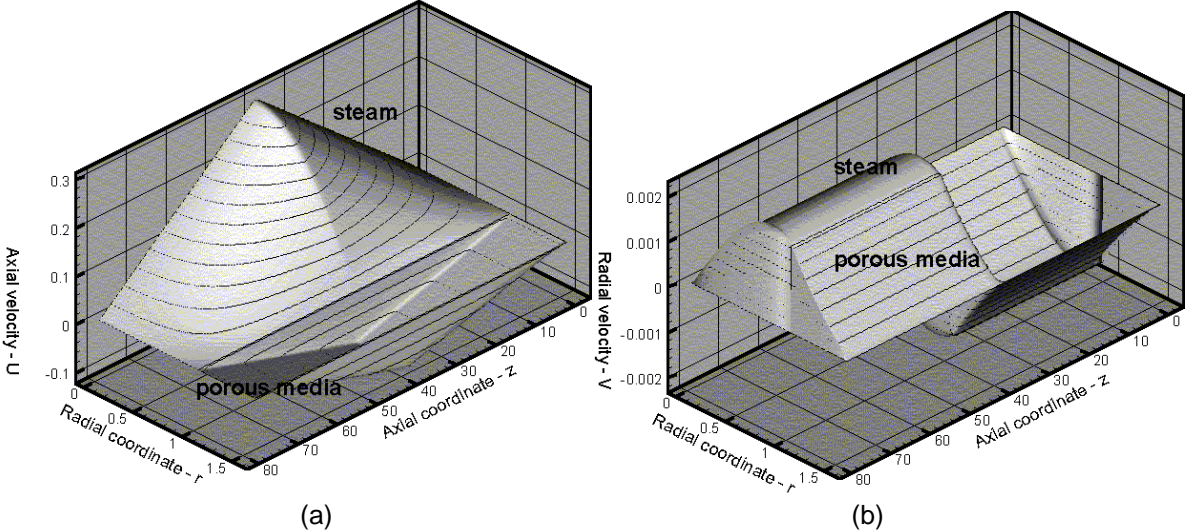


Figure 7. Velocity fields, $\Omega = 0$: (a) axial - U , (b) radial - V .

Figure 8 shows temperature profiles in the case where the temperature is close to the limit (Fig. 8.a) and when it has passed away (Fig. 8.b). The variation observed in temperature profile was a more smooth variation when crossing the interface section from the negative to the positive heat flux. It was also observed that maximum temperature does not depends on the angular speed, since the process occurs in steady state and the whole vapor is at the saturation temperature. Fig. 9 shows the variation of maximum heat pipe temperature against heat flux. The increasing of curve inclination demonstrates the point when the heat pipe capacity is not enough to avoid the increasing of sensible heat exchanged to the fluid, which is much below than the point where the recirculations will block the heat pipe.

Finally, the results presented by Miranda (1998) for the limit of angular speed as a function of the wall heat flux in a specific cylindrical heat pipe were verified and extended for a general curve, relating the angular Reynolds number ($Re_{angular} = \Omega r_i / v_{vapor}$) to the injection

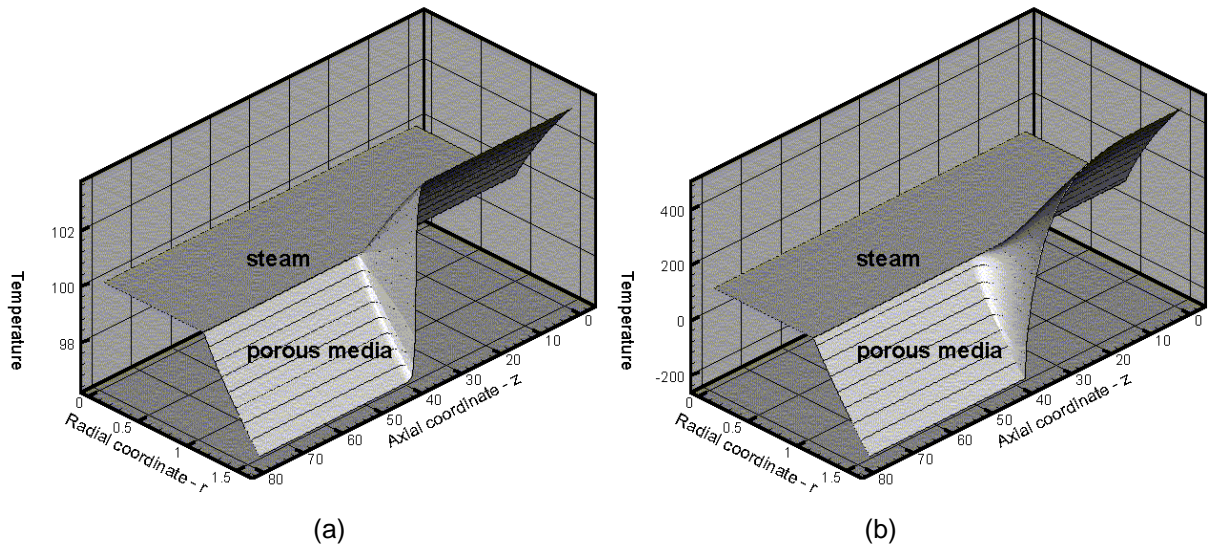


Figure 8. Temperature profiles, (a) $\Omega = 60, Q = 10^4$, (b) $\Omega = 100, Q = 10^5$.

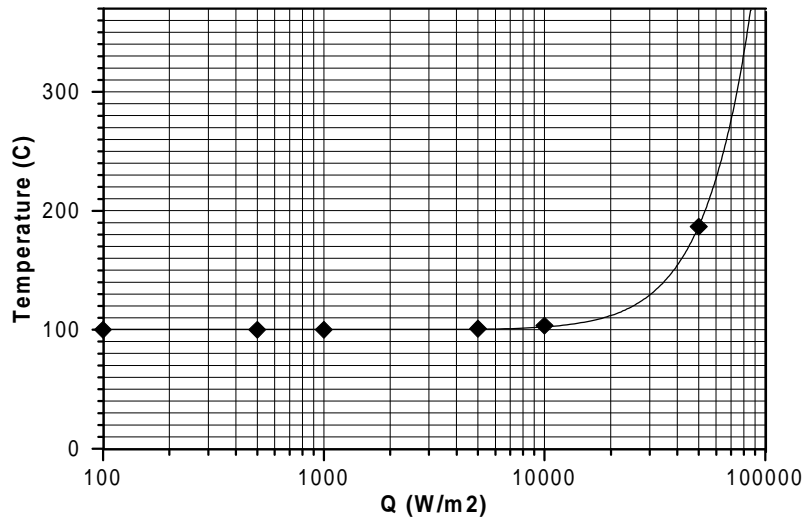


Figure 9. Maximum temperature in the porous region as a function of heat flux.

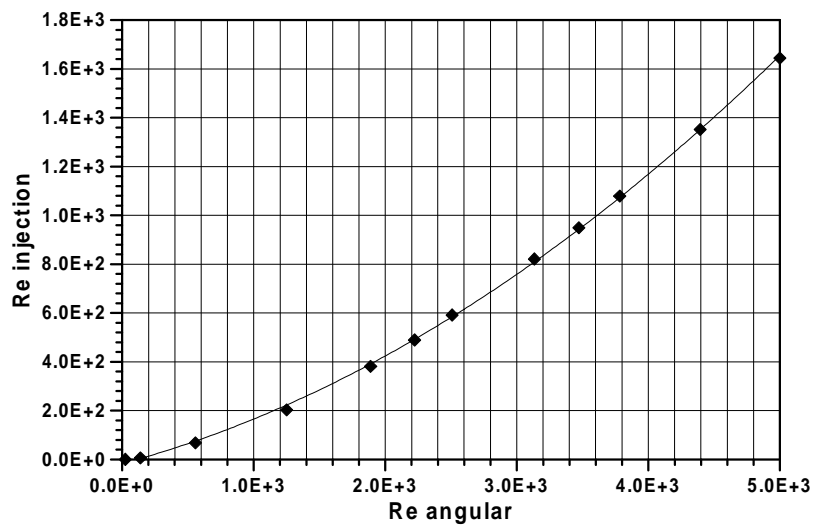


Figure 10. Limiting of cylindrical heat pipe operation.

Reynolds number ($Re_{injection} = V_i^*L/v_{vapor}$, where $V_i^* = Q/(\rho_{vapor} H)$ is the reference injection velocity). The curve, showed in Figure 10, can be extended to any cylindrical heat pipe, since the physical model is the same, and could be very useful in heat pipe design and operation.

4. CONCLUSION

In this work, the operation of rotating cylindrical heat pipes under critical conditions of wall heat flux and angular velocity were studied. In both cases, the main effect is the presence of recirculation cells, which grows and multiplies as the conditions become more critical. Such cells reduce the efficiency of heat pipe, since the vapor there cannot take part of the thermal cycle. The inferior limit of operation is a function of the recirculation growth, until the interruption of the fluid circulation in the tube, yielding the tube operation collapse. The upper limit of operation is related to the heat fluxes, but is controlled by the maximum temperature of the porous region, that does not depends on the rotation. Two curves are presented, which can be used for rotating heat pipe design.

Acknowledgements

The authors would like to acknowledge to FAPEMIG – The Scientific Sponsor Agency of the state of Minas Gerais - for the financial support provided for this work.

REFERENCES

- Daniels, T. C. & Al-Jumaily, F. K., 1975, Investigations of the Factor Affecting the Performance of a Rotating Heat Pipe, *Int. J. Heat & Mass Transfer*, 18, pp 691-973.
- Daniels, T. C. & Willians, R. J., 1978, Experimental Temperature Distribution and Heat Load Characteristics of Rotating Heat Pipes, *Int. J. Heat & Mass Transfer*, 21, pp 193-201.
- Daniels, T. C. & Willians, R. J., 1979, The Effect of External Boundary Conditions on Condensation Heat Transfer in Rotating Heat Pipes, *Int. J. Heat & Mass Transfer*, 22, pp 1237-1241.
- Faghri, A., Gogineni, S. and Thomas, S., 1993, Vapor Flow Analysis of Axially Rotating Heat Pipe, *Int. J. Heat & Mass Transfer*, 36(9), pp 2293-2303.
- Harley, C. & Faghri, A., 1995, Two-dimensional Rotating Heat Pipe Analysis, *Trans. ASME - J. Heat Transfer*, 117, pp 202-208.
- Ismail, K. A. R. & Miranda, R. F., 1988, Theoretical Analysis of a Rotating Heat Pipe, IHPS, Tsukuba, Japão, pp 157-162.
- Ismail, K. A. R. & Miranda, R. F., 1997, Two-dimensional Axisymmetrical Model for a Rotating Porous Wicked Heat Pipe, *Applied Thermal Engineering* 17(2), pp 135-155.
- Machado, H. A. & Miranda, R. F., 2000, Análise da Eficiência de Tubos de Calor Rotativos, Congresso Nacional de Engenharia Mecânica, Natal, Brazil, to appear.
- Miranda, R. F., 1998, Desempenho de Tubos de Calor Rotativos com Distribuição Qualquer de Calor no Evaporador, Congresso Norte-Nordeste de Engenharia Mecânica, Fortaleza, Brazil, pp 103-110.